Jurnal Teknologi

Full Paper

A SYNCHRONIZATION LOSS DETECTION METHOD FOR PMSM SPEED SENSORLESS CONTROL

Bernadeta Wuri Harini, Faiz Husnayain, Aries Subiantoro, Feri Yusivar*

Electrical Engineering, Universitas Indonesia, Kampus UI Depok 16424, West Java, Indonesia

Article history
Received
1 November 2019
Received in revised form
20 April 2020
Accepted
30 April 2020
Published online
22 June 2020

*Corresponding author
feri.yusivar@ui.ac.id

Graphical abstract

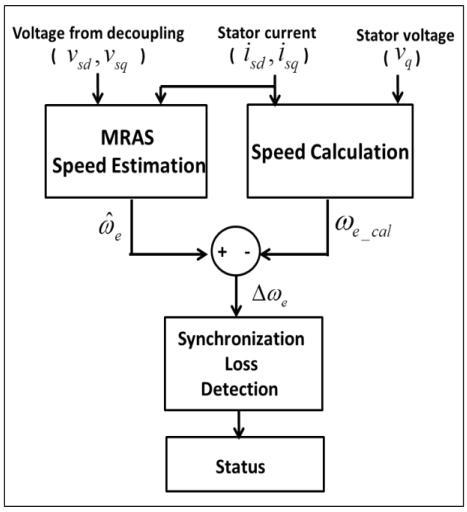

Abstract

Permanent Magnet Synchronous Motor (PMSM) is an AC motor in which the rotor must operate at synchronous speed in all load conditions. If the motor mechanical load increases, the motor can lose synchronization, stopping the motor. In sensorless control systems, i.e., those without speed sensors, the speed is estimated from the stator current using the Model Reference Adaptive System (MRAS) algorithm. Because such systems therefore cannot detect the loss of synchronization, it is necessary to design a synchronization loss detection system. Here, another speed estimation calculated from the stator currents and voltages is introduced. The speed is called a calculated speed. In the normal condition (synchronous condition), estimated speed and calculated speed will be approximately equal. However, when synchronization loss occurs, these two speed values diverge. On the basis of this phenomenon, a synchronization loss detection algorithm and method are developed. The algorithm's speed-delta boundary values and detection period must be determined. The greater the setpoint speed, the higher the speed-delta boundary values but the smaller the detection period. The experiments confirm that the proposed algorithm is able to effectively detect the occurrence of synchronization loss

Keywords: Control, sensorless, detection, synchronization, load

1.0 INTRODUCTION

One type of AC motor is the Permanent Magnet Synchronous Motor (PMSM). PMSMs are widely used as a driving force for electric vehicles because of their efficiency, torque, power, and power factors, as well as their smaller sizes and lighter weights. In addition, PMSM produces relatively low current rates, vibration, and inertia vibrations [1].

A PMSM is a three-phase synchronous motor with a permanent magnet rotor surrounded by a stator in the form of a coil. The PMSM rotor rotates at the same speed as the stator magnetic field. The rotor is locked in the rotary field. The rotor must operate at synchronous speed in all load states. If the motor mechanical load increases, the motor can lose synchronization, causing the motor to stop running [2].

As DC motors, torque control in AC motors is achieved by controlling the motor currents. But unlike the case for DC motors, both the phase angle and the modulus of the current in AC motors must be controlled. In other words, the current vector has to be controlled [3]. Vector control allows the torque and flux that produce current to be decoupled so that each can be controlled separately. In this process, the three-phase PMSM mathematical model is converted to a two-phase mathematical model using the Clarke and Park transformation [3].

In the sensor-based control methods, a position/speed sensor mounted on the rotor would be required in order to control the speed of the motor. However, the addition of sensors increases costs and causes problems when installing sensors. To overcome difficulties in installing position/speed sensors, speed

sensorless control can be used. To estimate the speed value, an observer estimates the motor speed of the rotor current that is measured using a current sensor. There are several types of observers, among them the Model Reference Adaptive System (MRAS) [4] used in the present research.

In speed sensorless control systems in which the speed is estimated from stator current using the MRAS algorithm, a key problem is that the system is not able to detect synchronization loss that accompanies substantial increases in load, as illustrated [5] and experimentally demonstrated [6] by Harini *et al.* (2017, 2018). In their study, the load on the motor was increased substantially once motor rotation had stabilized at 90 RPM, so that it oscillated around speed 0 (i.e., the motor stopped). Although the load was then released again, the motor remained stopped; that is, the actual speed was zero. However, the estimated value of motor speed did not show a value of 0, instead remaining stable at a finite nonzero value. This means that an estimation error occurred. Such estimation error must be detected as early as possible so that the condition of synchronization loss can be prevented. Therefore, it is necessary to design a synchronization loss detection system.

Various researchers have proposed methods of control system error detection. Yusivar *et al.* (2014) proposed a smart household energy system algorithm to anticipate error conditions in the power system network [7]. This algorithm did not apply to sensorless systems. Foo *et al.* (2013) proposed an algorithm to detect faults in current sensors used in sensorless control systems of Interior PMSMs [8]. In contrast to the algorithm proposed in the present study, their algorithm was used to detect errors in either of the two current sensors installed. This algorithm thus did not detect speed estimation error directly. Bisheimer *et al*. (2008) also proposed methods of current sensor error detection [9]. Dybkowski *et al.* (2014) proposed a method for detecting position sensor errors in induction motors [10]. Most published methods related to error detection apply to induction motors [11-21].

In studies conducted by previous researchers, the motor was not tested for large loads. However, Barcaro *et al.* (2012) tested the Permanent Magnet engine under several load conditions; their results showed no synchronization loss for this engine [22]. Research conducted by SC Agarlita *et al.* [23] and H Wei *et al.* [24] also tested PMSM with several variations of the load but did not show synchronization loss. Therefore, the research in this paper has not been studied by other researchers.

In detecting motor position or speed errors in a sensorless control system, two inputs are commonly used. They are the stator current and voltage. Most of the detection methods use current input only. For example, in Torabi *et al.* (2017) and Consoli *et al.* (2010), the method of detecting position errors used a current sensor to detect the stator current [18], [25]. The method proposed in the present paper uses input from current and voltage sensors. Shaeboub *et al.* (2015) compared two methods of detecting stator errors, i.e. a method that uses input from the current sensor and a method that uses input from the voltage sensor [19]. Their results for speed sensorless control show that voltage sensor input provides effective diagnostic features. Therefore, to detect the loss of synchronization, here, another speed estimation calculated from the stator currents and voltages is introduced. The speed is called a calculated speed.

As for decision-making algorithms, several methods have been studied and applied to sensors. Yusivar *et al.* (2013) and Foo *et al*. (2013) directly compared the current from the current sensor with a certain boundary value [7], [8]. In contrast, in Strankowski and Guziński (2016), the decision is made by activating a timer that expires 100 s after a certain number of samples [17]. In the present study, decision making is done by activating a timer that expires several seconds after the first occurrence of a certain threshold of difference between the estimated speed and the calculated speed. The optimal timer duration is determined experimentally. Such a method is useful for anticipating pseudo-estimation errors, in which synchronization loss does not occur. In those scenarios, the estimated value may change slightly but then return to the previous value.

In this paper, the proposed synchronization loss detection method for PMSM speed sensorless control systems is implemented experimentally. To this end, the Myway PE-Expert4 Digital Control System is used [6].

2.0 METHODOLOGY

As explained in the introduction, a sensorless control system that uses MRAS as an observer is not able to detect synchronization loss that accompanies substantial increases in load. Therefore, in this paper, the new method of detecting synchronization loss is proposed. The proposed synchronization loss detection method system is shown in Figure 1.

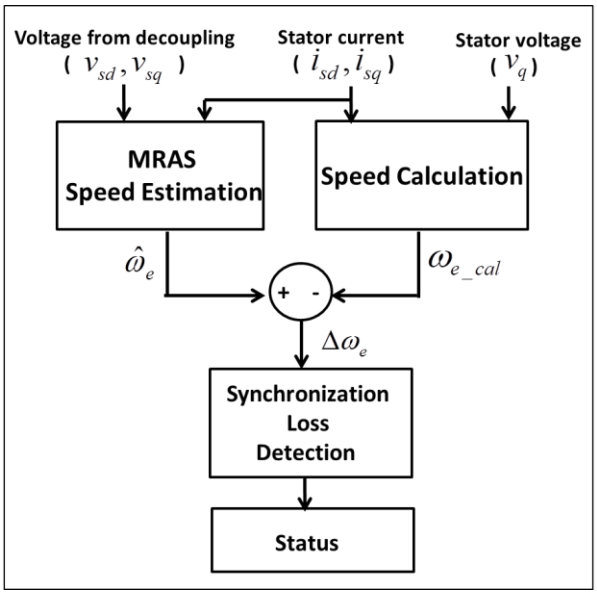

Figure 1 Proposed synchronization loss detection method

As shown in Figure 1, synchronization loss detection is determined on the basis of the speed-delta value ($\Delta\omega_e$), which is the difference between the estimated rotational speed ($\hat{\omega}_e$) and the calculated rotational speed (ω_{e_cal}). The calculated speed formula will be provided in detail below. The inputs of speed calculation are stator currents and voltages using sensors. The estimated speed is the output of the MRAS observer as part of the speed sensorless control system. The MRAS estimates the speed from stator currents measured using the current and voltage sensors from the decoupling part of the speed sensorless control system.

Figure 2 shows the proposed algorithm for synchronization loss detection. To determine synchronization loss, the speed-delta boundary values must be determined. That process is based on data obtained experimentally. If the speed-delta is outside the specified range (Delta ≥ Upper or Delta ≤ Lower), then timer dt2 is activated. Determination of dt2's duration (detection period), i.e., Delay_2, is also accomplished experimentally. If the speed-delta value continues to increase during dt2, then the status variable is marked "1". This means that there has been a synchronization loss that has caused motor rotation to stop, even while the observer estimates that the motor is still running at a certain speed. On the other hand, if the speed-delta value decreases during dt2, then the status variable is marked "0". This means no synchronization loss has occurred. To overcome inaccurate calculation due to transient conditions at the start of the motor, initiation of the error detection process is delayed by a delay period (Delay_1) as implemented by the activation of timer dt1. Determination of dt1's duration, i.e., Delay_1, is also done experimentally.

As explained above, the values in the algorithm, such as delta speed boundaries, Delay_1 (delay period) and Delay_2 (detection period), are determined experimentally. In Strankowski and Guziński (2016), the determination of the timer period activation, i.e., 100 s after a certain number of samples, was not explained [17]. Therefore, in this paper, the timer period activation was determined experimentally. The algorithm was tried for several periods, from large to small period, to get the best fault detection. If these values are too large then the system will be late in detecting synchronization losses. However, if these values are too small, the system can detect the synchronization loss incorrectly.

The synchronization loss detection mechanism used in the sensorless control system is shown in Figure 3. The system consists of two parts: the original sensorless control system [6] and the proposed synchronization loss detection system.

The sensorless control system consists of:

a. the motor used in this study, i.e., a PMSM with specifications as shown in Table 1,
b. the observer used in this study, i.e., an MRAS to estimate motor speed,
c. the current control used in this study, i.e., a Proportional Integral controller, and
d. the motor speed control used in this study, i.e., an Integral Proportional controller.

Observer and controller constants referring drawn from previous research can be found in Table 2 [6]. The constants consist of gain values of observer and controllers, current controller time constant (Tsc), and speed controller time sampling (Tss).

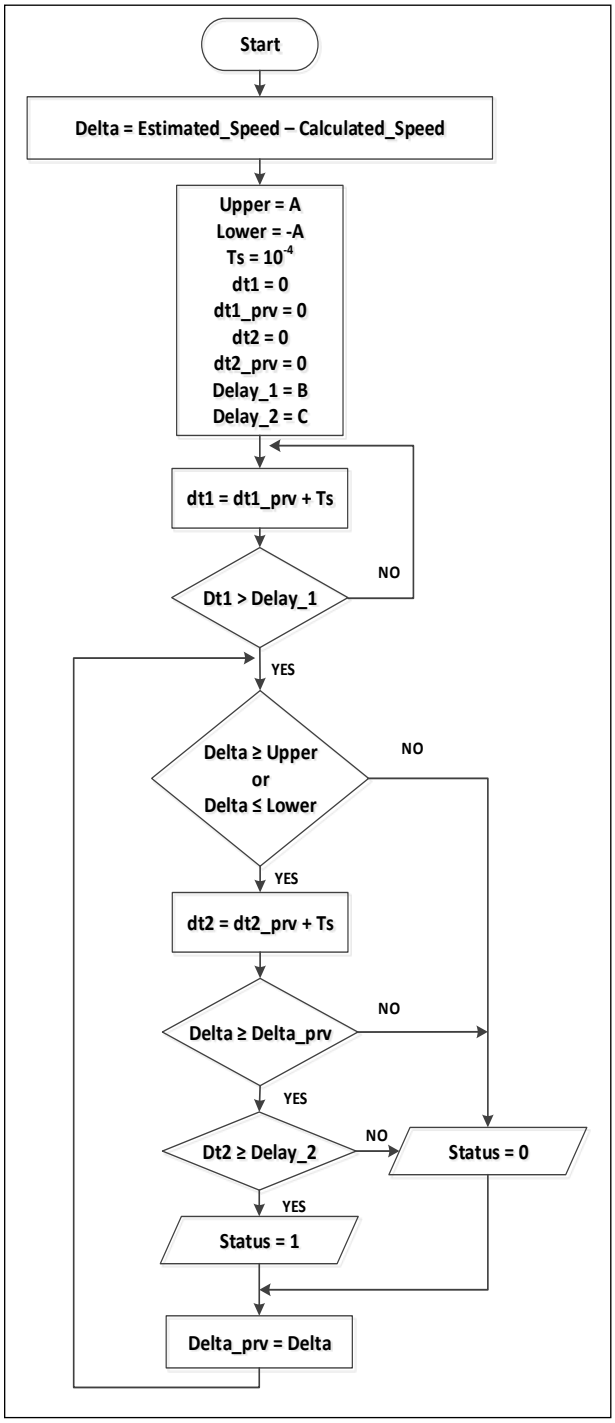

Figure 2 Algorithm for synchronization loss detection

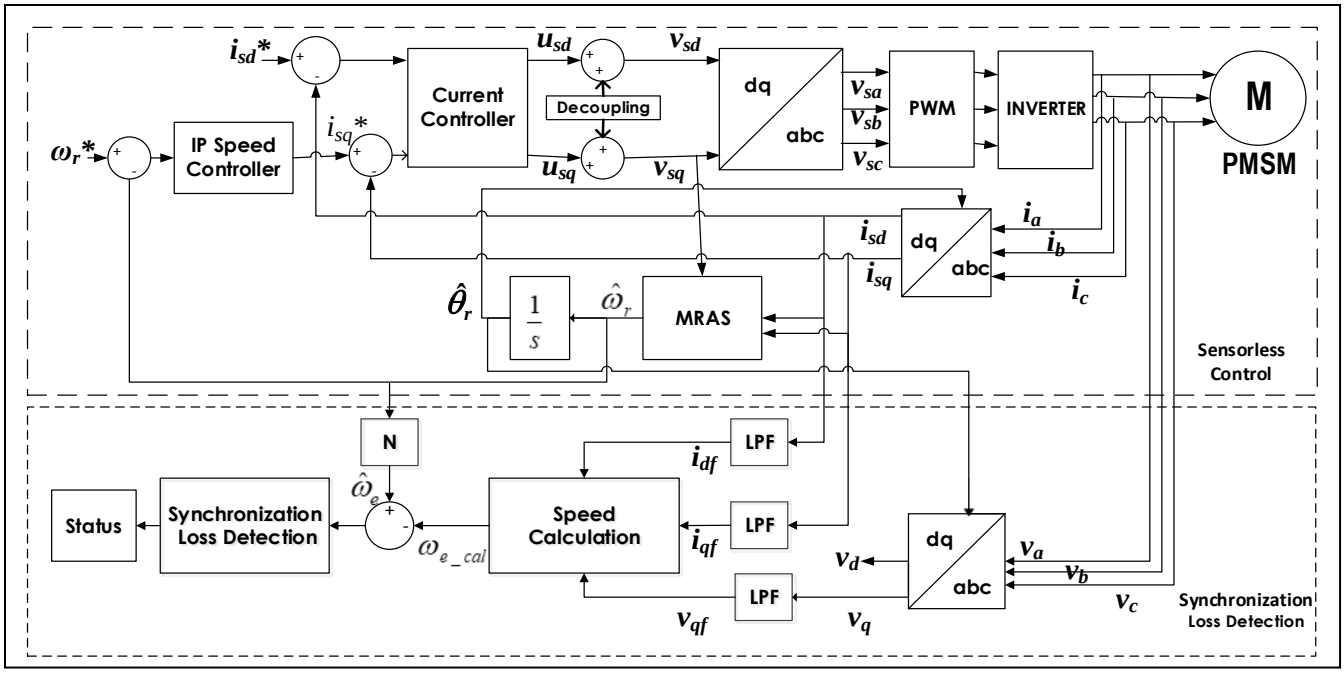

Figure 3 Block diagram of proposed synchronization loss detection mechanism for the PMSM sensorless control system

Table 1 PMSM specifications

No.	Parameters	Values
1	Number of pole pairs *N*	4
2	Stator resistance R_s (Ω)	0.14710
3	Stator inductance in the *d*-axis L_{sd} (mH)	0.29420
4	Stator inductance in the *q*-axis L_{sq} (mH)	0.38247
5	Electrical constant k_e (Vpeak/rad/s)	0.05597
6	Magnet flux linkage (ϕ_F) (Vpeak/rad/s/N)	0.0134
7	Motor inertia *J* (kgm²)	0.01

Table 2 Observer and controller constants

No.	Functions	Constants	Values
1	Current Controller	K_{pd}	29.420
		K_{id}	14.710
		K_{pq}	38.247
		K_{iq}	14.710
		T_{sc}	0.0001 s
2	Speed Controller	K_p	0.2125
		K_i	0.9
		T_{ss}	0.001 s
3	Observer	K_{wrp}	0.01
		K_{wri}	0.1

The synchronization loss detection system consists of:

a. current and voltage measurements using current and voltage sensors. The three-phase current and voltage measurements are then converted to two phases using the Clarke and Park transformation [26];
b. Low Pass Filter (LPF);
c. speed calculation; and
d. synchronization loss detection method.

The synchronization loss detection method has been explained above. Other parts of the synchronization loss detection system are explained below.

a. Current and Voltage Measurements

The three-phase mathematical model of PMSM is changed into a two-phase mathematical model using Clarke and Park transformations [26]. The Clarke transformation converts the balanced three-phase quantities ($v_{sa,sb,sc}$) into a two-phase stationary reference frame ($v_{s\alpha,s\beta,0}$) using (1):

$$\begin{bmatrix} v_{s\alpha} \\ v_{s\beta} \\ v_0 \end{bmatrix} = \sqrt{\frac{2}{3}} \begin{bmatrix} 1 & -\frac{1}{2} & -\frac{1}{2} \\ 0 & \frac{\sqrt{3}}{2} & \frac{-\sqrt{3}}{2} \\ \frac{1}{2} & \frac{1}{2} & \frac{1}{2} \end{bmatrix} \begin{bmatrix} v_{sa} \\ v_{sb} \\ v_{sc} \end{bmatrix} \quad (1)$$

where $\mathbf{v}_{s\alpha}$ and $\mathbf{v}_{s\beta}$ are the respective stator voltages in the $\boldsymbol{\alpha}$,$\boldsymbol{\beta}$ reference frame.

The Park transformation converts from a stationary reference frame into a rotating reference frame (***d***, ***q***, 0) using (2).

$$\begin{bmatrix} v_{sd} \\ v_{sq} \end{bmatrix} = \begin{bmatrix} \cos\theta_e & \sin\theta_e \\ -\sin\theta_e & \cos\theta_e \end{bmatrix} \begin{bmatrix} v_{s\alpha} \\ v_{s\beta} \end{bmatrix} \quad (2)$$

where θ_e is the electric angle of the motor, and $\mathbf{v}_{sd}$ and $\mathbf{v}_{sq}$ are the respective stator voltages in the ***d-q*** reference frame.

b. Low Pass Filter (LPF)

To reduce fluctuations in the values of the stator current and voltage that are measured, the current and voltage are filtered using the transfer function (3):

$$G_f(s) = \frac{1}{T_s s + 1} \tag{3}$$

where T_s is the time constant. As shown in Figure 4, a 100 ms time constant is able to reduce signal noise. Therefore, this study uses a time constant of 100 ms.

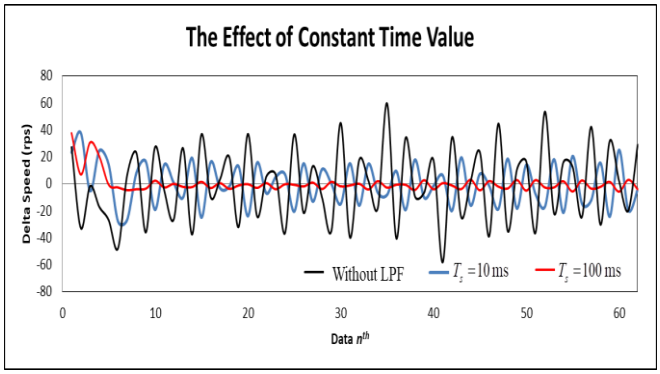

Figure 4 The effect of constant time value for speed-delta value ($\Delta\omega_e$)

c. Speed Calculation

Because a speed sensorless system does not measure rotor speed directly, another speed estimation in order to detect synchronization loss is introduced. This estimation is calculated from the stator currents and voltages and is called a calculated speed (ω_{e_cal}), as illustrated in Figure 1. In the normal condition (synchronous condition), estimated speed ($\hat{\omega}_e$) and calculated speed remain nearly equal. However, when synchronization loss occurs, these speed values diverge. Synchronization loss detection is algorithmically determined from the speed-delta ($\Delta\omega_e$), that is, the difference between estimated speed and calculated speed.

Motor speed is calculated on the basis of the PMSM mathematical model in the *d-q* frame explained in Harini *et al*. [27]. The PMSM model is:

$$\begin{bmatrix} v_{sd} \\ v_{sq} \end{bmatrix} = \begin{bmatrix} R_s + pL_{sd} & -N\omega_r L_{sq} \\ N\omega_r L_{sd} & R_s + pL_{sq} \end{bmatrix} \begin{bmatrix} i_{sd} \\ i_{sq} \end{bmatrix} + \begin{bmatrix} 0 \\ N\omega_r \phi_F \end{bmatrix} \tag{4}$$

where **p** is **d/dt**, i_{sd} is the stator current on the ***d***-axis, i_{sq} is the stator current on the ***q***-axis, R_s is the stator resistance, L_s is the stator inductance, ***N*** is the number of pole pairs, ω_r is the rotor speed, and ϕ_F is the magnet flux linkage. Equation (4) can then be restated as:

$$\frac{d}{dt} i_{sd} = \frac{V_{sd} - R_s i_{sd} + N\omega_r L_{sq} i_{sq}}{L_{sd}} \tag{5}$$

$$\frac{d}{dt} i_{sq} = \frac{V_{sq} - i_{sd} N\omega_r L_{sd} - R_s i_{sq} - N\omega_r \phi_F}{L_{sq}} \tag{6}$$

If Equation (6) is used and the inputs obtained from the LPF, then Equation (6) becomes Equation (7):

$$\frac{d}{dt} i_{qf} = \frac{V_{qf} - i_{df} N\omega_{rf} L_{sd} - R_s i_{qf} - N\omega_{rf} \phi_F}{L_{sq}} \tag{7}$$

where i_{df} is the filtered stator current on the ***d***-axis, i_{qf} is the filtered stator current on the ***q***-axis, L_{sd} is the stator inductance on the ***d***-axis, L_{sq} is the stator inductance on the ***q***-axis, and ω_{rf} is the rotor speed.

In steady-state, *i.e.*, $\frac{d}{dt} i_{qf} = 0$, then the electric motor rotational speed calculation result is given by:

$$\omega_{e\_cal} = N\omega_{rf} = \frac{V_{qf} - R_s i_{qf}}{i_{df} L_{sd} + \phi_F} \tag{8}$$

Finally, the electric torque of the PMSM is given by:

$$T_e = N\left\{\phi_F i_{sq} + \left(L_{sd} - L_{sq}\right) i_{sd} i_{sq}\right\} \tag{9}$$

Figure 5 shows the synchronization loss testing system. A PMSM equipped with brakes is connected to the inverter. A Myway PE-Expert4 Digital Control System is used to control motor speed. The system is equipped with a monitoring system so that it can display motor data. To find out the actual rotor speed, the system is equipped with an Autonics Incremental Rotary Encoder E40HB10-1024-6-L-5 type as a sensor.

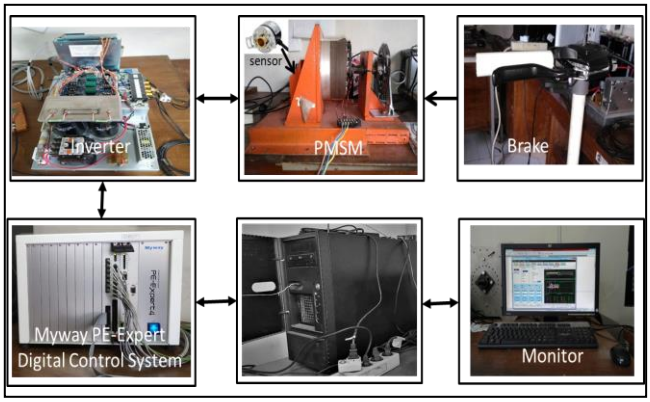

Figure 5 Implementation system

3.0 RESULTS AND DISCUSSION

The results of the proposed synchronization loss detection method can be seen in Figures 6 and 7. Figure 6 shows the estimated speed and calculated speed in a normal condition, i.e., synchronous condition. Figure 7 shows the estimated speed and calculated speed before and after a substantial load causes synchronization loss.

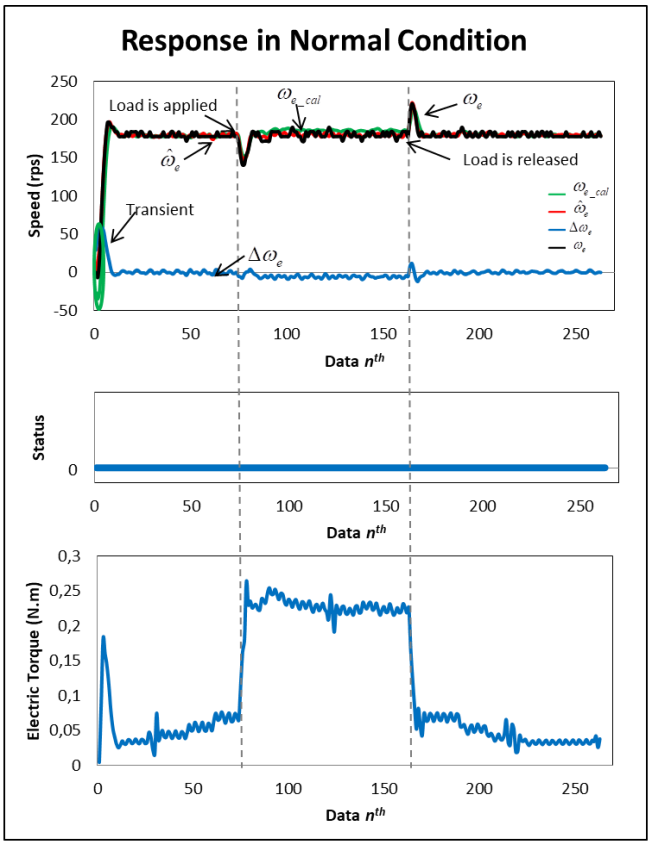

Figure 6 Response of PMSM in normal condition

From Figure 6, it is known that in the normal condition (synchronous condition), estimated speed ($\hat{\omega}_e$) and calculated speed remain nearly equal. Although some oscillations occur when the motor is loaded, the motor speed returns to its setpoint value, i.e., ω_r^* = 45 rps (with $\omega_e^* = N \times \omega_r^*$ = 180 rps). However, when synchronization loss occurs, these speed values diverge, as shown in Figure 7. It appears that when the motor substantially loaded above 100% by braking the rotor until it stops (ω_e dropping to a value of 0 and oscillating there), the MRAS observer fails to indicate this state. Although the estimated speed value ($\hat{\omega}_e$) did drop slightly when the motor was loaded, the estimated speed then returned to the previously estimated speed value, even though the actual condition of the rotor was stopped. This estimate diverges from the calculated speed value (ω_{e_cal}). It appears that the calculated speed value is able to show changes in speed according to actual conditions. It can be concluded that the calculated speed value can be used as an acknowledgment of synchronization loss. In both figures, the PMSM electric torque value (T_e) is calculated using Equation (9).

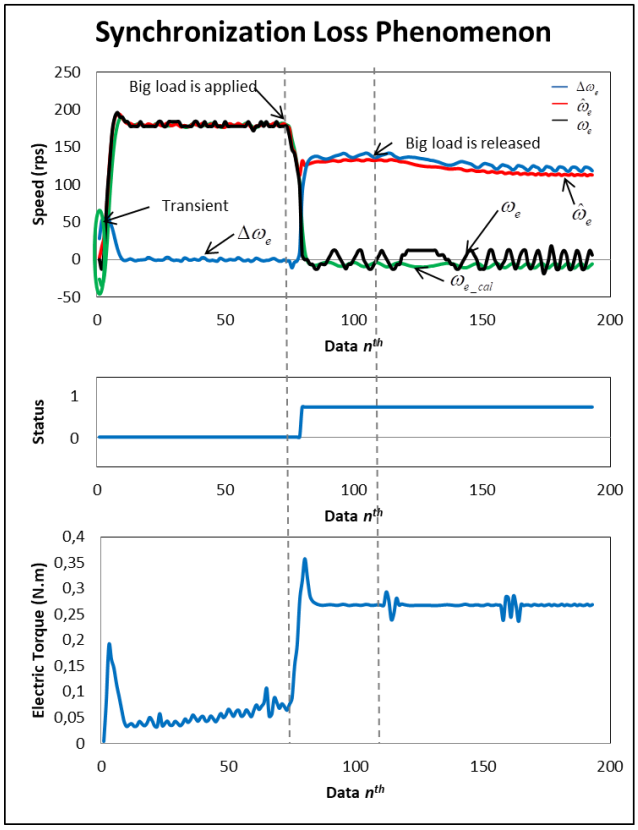

Figure 7 Synchronization loss detection at speed 180 revolutions per second

As explained above, synchronization loss is determined from the speed-delta ($\Delta\omega_e$), i.e., the divergence between the estimated speed and calculated speed. It appears in Figure 7 that when synchronization loss occurs, the speed-delta value increases rapidly. Therefore, the speed-delta value can be used as an acknowledgment of synchronization loss. As shown in Figures 6 and 7, speed-delta values oscillate at transient conditions when motor rotation initiates. The delta speed boundaries value used in Figures 6 and 7 is ± 30 rps, while the delay period used is 0.5 seconds. The detection period used in both figures is 0.001 seconds. The values are shown in Table 3. Besides, the variable values (speed-delta boundary values, detection periods, and delay durations) used for the other set point speeds are also shown in Table 3, i.e. ω_e^* = 100, 120, 140, and 160 revolutions per second (rps).

From Table 3, it appears that the speed-delta boundary values are greater for higher setpoint speeds, since speed-delta fluctuations also are greater for higher setpoint speeds. This behavior is inversely proportional to that of detection period. It appears in Table 3 that the greater the setpoint motor speed, the shorter the detection period. For all setpoint speeds, the initiation of the synchronization loss detection algorithm was delayed for 0.5 s.

The delay period and detection period values stated in Table 3 were determined experimentally, as explained in the methodology section. The algorithm was tried for several period values until it got the best values, as shown in Table 3. These period values depend on the setpoint speed, as explained above.

Table 3 Variable values for synchronization loss detection

No.	Speed (rps)	Delay period (s)	Boundaries (rps)	Detection period (s)
1	100	0.5	±10	0.2
2	120	0.5	±15	0.15
3	140	0.5	±20	0.1
4	160	0.5	±25	0.05
5	180	0.5	±30	0.001

*rps = revolutions per second

4.0 CONCLUSIONS

In this paper, the loss of synchronization in a sensorless control system on a PMSM because of a big load (above 100%) has been successfully detected by a novel synchronization loss detection algorithm. Detection is determined by the divergence between the estimated speed and the speed calculated from the stator current and stator voltage. By selecting speed-delta boundary values and the correct detection period, this synchronization loss detection system works well to prevent synchronization loss. In future work, this system's detection results will be used as an input to the speed sensorless system. This input will allow the speed sensorless system to overcome synchronization loss so that the motor can operate normally.

Acknowledgment

This research is supported by Lembaga Pengelola Dana Pendidikan (LPDP) grant.

References

[1] M. Yilmaz. 2015. Limitations/Capabilities of Electric Machine Technologies and Modeling Approaches for Electric Motor Design and Analysis in Plug-in Electric Vehicle Applications. *Renewable and Sustainable Energy Reviews.* 52: 80-99.
DOI: https://doi.org/10.1016/j.rser.2015.07.033.

[2] Park and D.-H. Lee. 2019. Sensorless Control of PMSM using Voltage and Current Angle Estimation. *22nd International Conference on Electrical Machines and Systems (ICEMS), 2019*. Harbin, China, 11–14 August 2019. 1-5.
DOI: https://doi.org/10.1109/ICEMS.2019.8922294.

[3] P. Vas. 1998. *Sensorless Vector and Direct Torque Control.* Oxford University Press, USA.

[4] F. Semiconductor. 2008. Sensorless PMSM Vector Control with a Sliding Mode Observer for Compressors Using MC56F8013. Document Number.

[5] B. W. Harini, N. Avianto, and F. Yusivar. 2018. Effect of Initial Rotor Position on Rotor Flux Oriented Speed Permanent Magnet Synchronous Motor Control using Incremental Encoder. *Proceeding in 2018 2nd International Conference on Smart Grid and Smart Cities (ICSGSC)*. 95-99.
DOI: https://doi.org/10.1109/ICSGSC.2018.8541305.

[6] B. W. Harini, A. Subiantoro, and F. Yusivar. 2017. Study of Speed Sensorless Permanent Magnet Synchronous Motor (PMSM) Control Problem Due to Braking During Steady State Condition. *Proceeding in Quality in Research (QiR): International Symposium on Electrical and Computer Engineering, 2017 15th International Conference on*. 184-189.
DOI: https://doi.org/10.1109/QIR.2017.8168479.

[7] F. Yusivar, R. Suryadiningrat, A. Subiantoro, and R. Gunawan. 2014. Single Phase PV Grid-Connected in Smart Household Energy System with Anticipation on Fault Conditions. *International Journal of Power Electronics and Drive Systems*. 4: 100.
DOI: https://doi.org/10.11591/ijpeds.v4i1.5368.

[8] G. H. B. Foo, X. Zhang, and D. M. Vilathgamuwa. 2013. A Sensor Fault Detection and Isolation Method in Interior Permanent-magnet Synchronous Motor Drives Based on an Extended Kalman Filter. *IEEE Transactions on Industrial Electronics.* 60: 3485-3495.
DOI: https://doi.org/10.1109/TIE.2013.2244537.

[9] G. Bisheimer, C. De Angelo, J. Solsona, and G. Garcia. 2008. Sensorless PMSM Drive with Tolerance to Current Sensor Faults. *Proceeding in 2008 34th Annual Conference of IEEE Industrial Electronics.* 1379-1384.
DOI: https://doi.org/10.1109/IECON.2008.4758155.

[10] M. Dybkowski, K. Klimkowski, and T. Orlowska-Kowalska. 2014. Speed Sensor Fault Tolerant Direct Torque Control of Induction Motor Drive. *Proceeding in 2014 16th International Power Electronics and Motion Control Conference and Exposition.* 679-684.
DOI: https://doi.org/10.1109/EPEPEMC.2014.6980574.

[11] M. E. H. Benbouzid, D. Diallo, and M. Zeraoulia. 2007. Advanced Fault-tolerant Control of Induction-motor Drives for EV/HEV Traction Applications: From Conventional to Modern and Intelligent Control Techniques. *IEEE Transactions on Vehicular Technology*. 56: 519-528.
DOI: https://doi.org/10.1109/TVT.2006.889579.

[12] M. Romero, M. Seron, and J. De Dona. 2010. Sensor Fault-Tolerant Vector Control of Induction Motors. *IET Control Theory & Applications.* 4: 1707-1724.
DOI: https://doi.org/10.1049/iet-cta.2009.0464.

[13] K. Rothenhagen and F. W. Fuchs. 2009. Current Sensor Fault Detection, Isolation, and Reconfiguration for Doubly Fed Induction Generators. *IEEE Transactions on Industrial Electronics.* 56: 4239-4245.
DOI: https://doi.org/10.1109/TIE.2009.2017562.

[14] S. Karimi, A. Gaillard, P. Poure, and S. Saadate. 2009. Current Sensor Fault-tolerant Control for WECS with DFIG. *IEEE Transactions on Industrial Electronics*. 56: 4660-4670.
DOI: https://doi.org/10.1109/TIE.2009.2031193.

[15] T. A. Najafabadi, F. R. Salmasi, and P. Jabehdar-Maralani. 2010. Detection and Isolation of Speed-, DC-link Voltage-, and Current-sensor Faults based on an Adaptive Observer in Induction-motor Drives. *IEEE Transactions on Industrial Electronics.* 58: 1662-1672.
DOI: https://doi.org/10.1109/TIE.2010.2055775.

[16] H. Berriri, M. W. Naouar, and I. Slama-Belkhodja. 2011. Easy and Fast Sensor Fault Detection and Isolation Algorithm for

Electrical Drives. *IEEE Transactions on Power Electronics.* 27: 490-499.
DOI: https://doi.org/10.1109/TPEL.2011.2140333.

[17] P. Strankowski and J. Guziński. 2016. Sensorless Fault Detection of Induction Motor with Inverter Output Filter. *Progress in Applied Electrical Engineering (PAEE)*. 1-6.
DOI: https://doi.org/10.1109/PAEE.2016.7605104.

[18] N. Torabi, V. M. Sundaram, and H. A. Toliyat. 2017. On-line Fault Diagnosis of Multi-phase Drives using Self-recurrent Wavelet Neural Networks with Adaptive Learning Rates. *Proceeding in 2017 IEEE Applied Power Electronics Conference and Exposition (APEC)*. 570-577.
DOI: https://doi.org/10.1109/APEC.2017.7930751.

[19] A. Shaeboub, S. Abusaad, N. Hu, F. Gu, and A. D. Ball. 2015. Detection and Diagnosis of Motor Stator Faults using Electric Signals from Variable Speed Drives. *Proceeding in 2015 21st International Conference on Automation and Computing (ICAC)*. 1-6.
DOI: https://doi.org/10.1109/IConAC.2015.7313938.

[20] M. Trabelsi and M. Boussak. 2014. Sensorless Speed Control of VSI-fed Induction Motor Drive under IGBT Open-switch Damage: Performances and Fault Tolerant Analysis. *Proceeding in 2014 International Conference on Electrical Sciences and Technologies in Maghreb (CISTEM)*. 1-8.
DOI: https://doi.org/10.1109/CISTEM.2014.7368727.

[21] M. Nemec, K. Drobnic, D. Nedeljkovic, R. Fiser, and V. Ambrozic. 2009. Detection of Broken Bars in Induction Motor through the Analysis of Supply Voltage Modulation. *IEEE Transactions on Industrial Electronics*. 57: 2879-2888.
DOI: https://doi.org/10.1109/TIE.2009.2035991.

[22] M. Barcaro, A. Faggion, N. Bianchi, and S. Bolognani. 2012. Sensorless Rotor Position Detection Capability of a Dual Three-phase Fractional-slot IPM Machine. *IEEE Transactions on Industry Applications.* 48: 2068-2078.
DOI: https://doi.org/10.1109/TIA.2012.2226222.

[23] S.-C. Agarlita, C.-E. Coman, G.-D. Andreescu, and I. Boldea. 2013. Stable V/f Control System with Controlled Power Factor Angle for Permanent Magnet Synchronous Motor Drives. *IET Electric Power Applications*. 7: 278-286.
DOI: https://doi.org/10.1049/iet-epa.2012.0392.

[24] H. Wei, H. Tao, F. Duan, Y. Zhang, Y. Li, and Z. Luo. 2018. Sensorless Current Model Control for Permanent Magnet Synchronous Motor based on IPID with Two-dimensional Cloud Model Online Optimization. *IET Power Electronics.* 12: 983-993.
DOI: ttps://doi.org/10.1049/iet-pel.2018.5892.

[25] A. Consoli, A. Gaeta, G. Scarcella, G. Scelba, and A. Testa. 2010. HF Injection-based Sensorless Technique for Fault-tolerant IPMSM Drives. *Proceeding in 2010 IEEE Energy Conversion Congress and Exposition*. 3131-3138.
DOI: https://doi.org/10.1109/ECCE.2010.5618459.

[26] A. Glumineau and J. de León Morales. 2015. *Sensorless AC Electric Motor Control.* Springer.
DOI: https://doi.org/10.1007/978-3-319-14586-0.

[27] B. W. Harini, A. Subiantoro, and F. Yusivar. 2017. Stability Analysis of MRAS Speed Sensorless Control of Permanent Magnet Synchronous Motor. *Proceeding in 2017 International Conference on Sustainable Energy Engineering and Application (ICSEEA), 2017*. 34-40.
DOI: https://doi.org/10.1109/ICSEEA.2017.